Available online at www.sciencedirect.com

SCIENCE DIRECT®

ACADEMIC PRESS

Journal of Sound and Vibration 265 (2003) 489–506

JOURNAL OF SOUND AND VIBRATION

www.elsevier.com/locate/jsvi

Experimental validation of a collocated PVDF volume velocity sensor/actuator pair

K. Henrioulle, P. Sas*

Department of Mechanical Engineering—PMA, Katholieke Universiteit Leuven, Celestijnenlaan 300B, B-3001 Leuven, Belgium

Received 2 July 2001; accepted 26 June 2002

Abstract

The active control of sound transmission through a rectangular panel is experimentally verified. The control system is based on a collocated volume velocity sensor/actuator pair which measures and excites the first radiation mode of the panel. Suppression of the first radiation mode is an efficient strategy to control the low frequency sound radiation from the panel. This configuration leads to a simple single-input single-output control system, to which feedback control can be applied.

Two implementations of the volume velocity sensor/actuator pair are tested. First, a polyvinyledene fluoride polymer (PVDF) volume velocity actuator foil with shaped electrodes is used in combination with an identical PVDF volume velocity sensor foil. Due to the mechanical coupling between the PVDF sensor and actuator foil, it is shown that a direct velocity feedback control scheme is not feasible because higher order structural modes will be destabilized. Instead integral force feedback is applied, such that the open-loop transfer function has a roll-off towards higher frequencies. Experiments show that this control strategy results in a reduction of the sound pressure in the receiving room of 10 dB at the first structural resonance without spillover to higher order modes. Due to the roll-off towards high frequencies, the control over higher order modes remains limited. Second, a discrete volume velocity sensor is constructed by summing the signals from 12 point sensors placed on the panel. The volume velocity actuator consists of two PVDF foils, glued on each side of the panel and driven in opposite phase. Direct volume velocity feedback is applied to this system, which is minimum phase. This control system is capable of reducing the sound pressure in the receiving room below 300 Hz by 10–15 dB without spillover to higher order modes.

*Corresponding author.
E-mail address: paul.sas@mech.kuleuven.ac.be (P. Sas).

0022-460X/03/$ - see front matter
doi:10.1016/S0022-460X(02)01559-6

1. Introduction

The control of low frequency sound transmission through a light weight panel partition cannot be realized with passive means. Active structural acoustic control, using structural actuators and sensors to control an acoustic cost function, can improve the low frequency sound transmission loss with a limited increase of the mass of the partition. Instead of using a multiple-input multiple-output control system with a model-based feedback control, this paper suggests a single-input single-output system with a collocated control system to achieve the same goal.

Borgiotti [1] introduced the concept of radiation modes for characterizing the exterior acoustic radiation from a vibrating structure. The radiation modes are a set of velocity distributions of the structure that radiate the sound power independently. The first radiation mode is a combination of structural modes associated with a volumetric component [2]. At low frequencies it resembles a piston-like motion of the panel, and thus is the most efficient radiating mode. Measuring the amplitude of this mode is equivalent to measuring the net volume velocity of the surface [3], and is therefore also named the volume velocity mode.

Several studies have used the concept of radiation modes for the implementation of active noise control systems.

Berkhoff [4] implemented a radiation mode sensor as a grid of structural point sensors. The first radiation mode, as well as higher order radiation modes can be sensed and minimized by this control system.

A distributed radiation mode sensor for a beam with different boundary conditions was simulated and implemented by Guigou et al. [5]. A polyvinyledene fluoride polymer (PVDF) sensor is shaped to measure the volume velocity of the beam.

Charette et al. [6] developed a PVDF volume displacement sensor based on the measured mode shapes of a clamped rectangular panel. The sensor consists of two narrow strips, one extending in the x-direction and the other in the y-direction.

Snyder et al. [7] constructed three PVDF radiation mode sensors to sense the first three radiation modes (termed transformed modes) of a panel. The sensors are implemented as one-dimensional sensors, stretching in the direction of the largest mode number and therefore show some sensitivity for higher order radiation modes. In a second paper, Snyder et al. [8] present a feedback control system for this configuration. Direct displacement feedback or velocity feedback is not successful because of the non-collocated nature of the radiation mode sensor(s) and point force actuator. The main problem is that the feedback gain has to be kept small to keep the system stable. An adaptive feedback control scheme yields good control results for impulse excitation of the system.

Johnson and Elliott [3] designed a distributed piezoelectric sensor foil to measure the amplitude of the volume velocity mode of a rectangular panel. This implementation is independent of the properties of the panel.

In another paper, Johnson and Elliott [9] simulated the active control of sound transmission through a panel and compared various sensing strategies. They conclude that reducing the volume velocity is a good strategy to control the sound power transmission through a panel at low frequencies, but in combination with a secondary point force or piezoceramic actuator large control spillover is noticed. This illustrates the need for a volume velocity actuator. The distributed volume velocity actuator foil is identical to the volume velocity sensor foil. The transfer function from the volume velocity actuator to the volume velocity sensor is minimum phase and an active control system built with this sensor/actuator pair will show no spillover to higher order radiation modes. Another advantage is that feedback control can be applied such that transient disturbances can be suppressed by this system.

The collocated PVDF volume velocity sensor/actuator pair was developed in the framework of the Brite–Euram project DAFNOR [10] by ISVR, Southampton University and is described by Gardonio et al. [11,12]. This paper deals with the experimental validation of the concepts presented in their work.

The panel partitions discussed in this paper have very small dimensions (300 mm × 400 mm). The sound transmission loss of panels of these dimensions is highly determined by the boundary conditions, and does not represent the sound transmission loss of a larger panel partition composed of the same material. Therefore, the sound transmission loss of the panel partitions is neither calculated nor measured. Instead the effect of the active control system is determined by measuring the sound pressure at a single point in the receiving room.

The paper is structured as follows. Section 2 develops a model for the vibration and sound radiation from the panel and discusses the control of volume velocity. Section 3 presents two implementations of the velocity sensor/actuator, as a PVDF volume velocity sensor/actuator pair and as a discrete volume velocity sensor in combination with a PVDF volume velocity actuator. Section 4 discusses the experimental results obtained with these configurations. Finally, Section 5 summarizes the main conclusions.

2. Active control of sound transmission

2.1. Sound transmission through a single panel partition

The single panel partition that will be used in this study is a clamped aluminium panel of $300 \times 400\,\mathrm{mm}^2$ and 1 mm thick. The vibration of the panel is described by an analytical model based on the classical plate equation, given in Ref. [13]:

$$\mathscr{L}_b w(x,y,t) + \rho_t h_t \ddot{w}(x,y,t) = f_m(x,y,t) + f_c(x,y,t), \tag{1}$$

in which

$$\mathscr{L}_b = D\left(\frac{\partial^4}{\partial x^4} + 2\frac{\partial^4}{\partial x^2 \partial y^2} + \frac{\partial^4}{\partial y^4}\right),$$

$$f_m(x,y,t) = F_m(x,y)\tilde{f}_m(t),$$

$$f_c(x,y,t) = F_c(x,y)\tilde{f}_c(t).$$

$\mathscr{L}_b$ is a differential stiffness operator for the bending motion, $w(x,y,t)$ is the out-of-plane displacement of the panel, ρ_t is the density of the panel, h_t is the panel thickness, D is the bending stiffness of the panel, $f_m(x,y,t)$ is the mechanical excitation or the disturbance force, $f_c(x,y,t)$ is the control force. In the case of a volume velocity actuator the latter represents a uniform force over the panel surface.

The partial differential equation (1) can be transformed into a set of algebraic equations using the expansion theorem [14]. Therefore, a solution for the displacement $w(x, y, t)$ has to be formed that satisfies the partial differential equation and the boundary conditions. This solution is of the form

$$w(x, y, t) = \sum_{b=1}^{\infty} W_b(x, y)\eta_b(t), \tag{2}$$

with $W_b(x, y)$ the mode shape and $\eta_b(t)$ the mode amplitude. Leissa [15] gives the solution for the mode shapes of a clamped rectangular panel.

The sound power output $\prod(\omega)$ of the panel is calculated based on the amplitudes of the structural modes [16]:

$$\prod(\omega) = \dot{\boldsymbol{\eta}}^H(\omega)\mathbf{M}(\omega)\dot{\boldsymbol{\eta}}(\omega), \tag{3}$$

where $\dot{\boldsymbol{\eta}}(\omega)$ is the matrix with the amplitudes of the modal velocities, $\mathbf{M}(\omega)$ is a matrix of structural mode radiation resistances. The eigenvalue decomposition of this matrix allows the calculation of the contribution of each radiation mode to the total sound power output of the panel. At low frequencies, the first radiation mode dominates the sound power radiation by the panel. This mode is excited by applying a uniform force over the panel surface. It is measured by integrating the velocity of the panel over the panel surface, which is equivalent to measuring the volume velocity of the panel.

The control approach envisaged in this paper aims at suppressing the first radiation mode of the panel. The control force is a uniform force over the panel surface with amplitude $\tilde{f}_c(t)$, exciting the volume velocity of the panel. The error signal is the volume velocity $\Phi(t)$ of the panel.

The analytical model is written in state space form as follows:

$$\begin{aligned} \dot{\mathbf{X}}_b(t) &= \mathbf{A}_b\mathbf{X}_b(t) + \mathbf{B}_{p,b}\tilde{f}_c(t) + \mathbf{B}_{m,b}\tilde{f}_m(t), \\ \Phi(t) &= \mathbf{C}_b\mathbf{X}_b(t) + \mathbf{D}_{p,b},\tilde{f}_c(t) + \mathbf{D}_{m,b}\tilde{f}_m(t). \end{aligned} \tag{4}$$

The states $\mathbf{X}_b(t)$ are the amplitudes of the modal displacement and velocity of the bending motion of the panel. The state space system (A_b, $\mathrm{B}_{p,b}$, C_b, $\mathrm{D}_{p,\mathrm{b}}$) represents the transfer function for the volume velocity sensor/actuator pair. The feedthrough matrices $\mathbf{D}_{p,\mathrm{b}}$ and $\mathbf{D}_{m,b}$ are zero.

2.2. Active control of volume velocity

The volume velocity sensor/actuator pair is collocated, and thus the transfer function, calculated by Eq. (4) has the characteristics as shown by the solid line in Fig. 1. Preumont [17] discusses the properties of a collocated sensor/actuator pair with respect to active damping control. The main characteristic is that between each pair of poles a zero is located. As a result the phase of the system is restricted to a band of -90° to $+90^\circ$.

The control scheme intended for this sensor/actuator pair is direct velocity feedback or an active increase of the structural damping. The feedback loop is closed such that $\tilde{f}_c(t) = -K\Phi(t)$ with K the feedback gain. The alternating pole–zero pattern yields a root locus that will never leave the stable left half-plane, as shown in Fig. 2. In the limit of an infinite feedback gain, the closed-loop poles reach the open-loop zeros and the output of the sensor is completely cancelled by pole–zero cancellation. The difference in frequency between the poles and the zeros of the

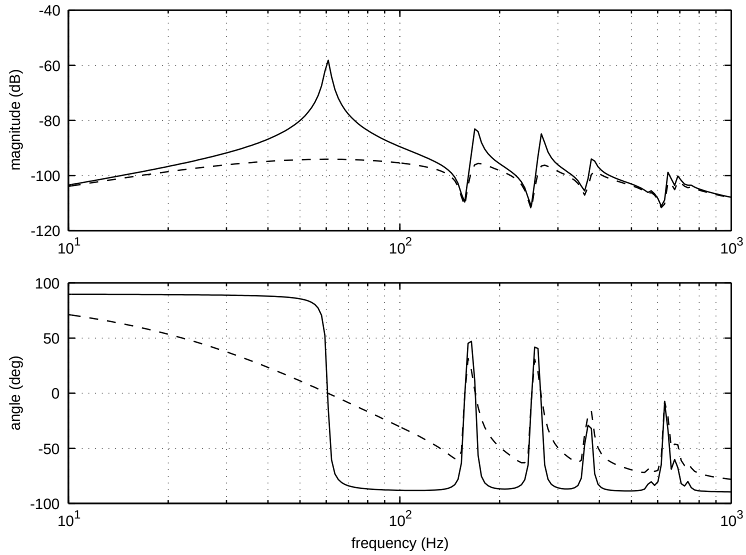

Fig. 1. Transfer function of the volume velocity sensor/actuator pair (solid line: without control, dashed line: with control).

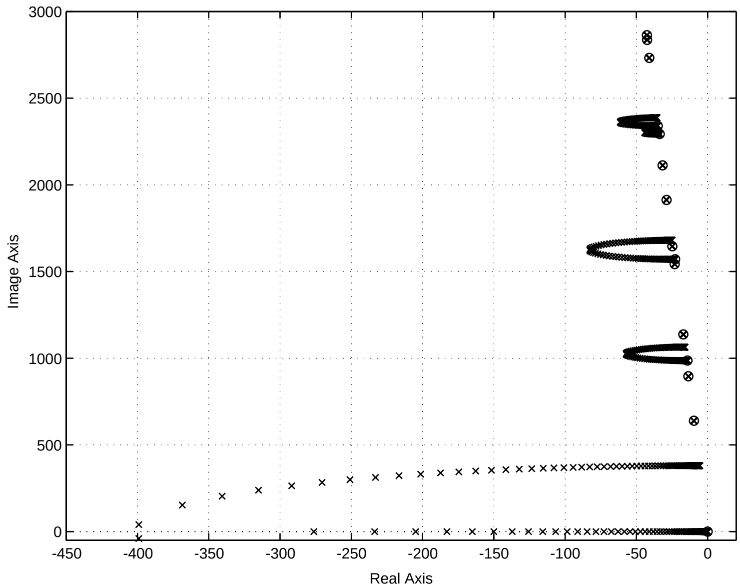

Fig. 2. Root locus plot of the ideal volume velocity sensor/actuator pair.

open-loop system determines how far the root locus will stretch in the left half-plane, and thus the maximum damping that can be achieved with velocity feedback. In the case of the active panel considered here, this distance is relatively small. Only for the first structural mode, a considerable active damping can be achieved. However, this observation is directly related to the control of the first radiation mode in which the first structural mode has a dominant contribution. The active damping achieved this way reduces the amplitude of the first radiation mode without altering the amplitude of the other radiation modes.

Fig. 1 shows the transfer function from volume velocity actuator to volume velocity sensor with control (dashed line). The gain was chosen such that the control force, which is proportional to the feedback gain, remains limited. The amplitude is reduced nicely below 300 Hz, and can be even further reduced by increasing the feedback gain.

3. Implementation of the volume velocity sensor/actuator

3.1. PVDF volume velocity sensor/actuator pair

This section discusses the implementation of a volume velocity sensor/actuator as a pair of PVDF foils with shaped electrodes. The aluminium panel is covered on its upper and lower surface with a PVDF foil of dimensions $300 \times 400\,\mathrm{mm}^2$ and 0.5 mm thickness [11]. One foil will be used as volume velocity sensor and the other as volume velocity actuator.

The spatial distribution of the control force $F_c(x, y)$ exerted on the panel by the piezoelectric actuator foil is given by [13]

$$F_c(x,y) = z_0\left\{\frac{\partial^2}{\partial x^2}(S(x,y)e_{31}) + 2\frac{\partial^2}{\partial x\partial y}(S(x,y)e_{36}) + \frac{\partial^2}{\partial y^2}(S(x,y)e_{32})\right\}, \tag{5}$$

with e_{31}, e_{32} and e_{36} the piezoelectric stress/charge constants, z_0 the distance of the neutral axis of the PVDF actuator foil to the neutral axis of the panel. $S(x, y)$ is the spatial sensitivity function of the PVDF foils given by [3]

$$S(x,y) = -\mu(x^2 - L_x x), \tag{6}$$

with μ a constant and L_x the length of the panel. This way $F_c(x, y)$ reduces to a constant, and the force exerted on the panel by the PVDF actuator is constant over the panel surface. As such only the first radiation mode is excited without control spillover to other radiation modes. The control force $\tilde{f}_c(t)$ is the voltage $V_3(t)$ applied to the actuator foil. An identical foil is used as a sensor. Its current output is proportional to the volume velocity of the panel [11,12].

In the derivation of the operation of the volume velocity sensor/actuator pair no assumptions are made on the geometrical or material properties of the panel. This contrasts with other implementations of modal sensors [18] or radiation mode sensors [4] that almost without exception depend on the geometrical or material properties of the structure they are applied to.

A schematic drawing of the aluminium panel equipped with the actuator and sensor foil is shown in Fig. 3. Around the PVDF foil, an edge of approximately 25 mm allows clamping of the panel. The two PVDF foils are identical, one of them is used as sensor and the other as actuator. The panel uses a structural actuator and structural sensor to control an acoustic cost function and is therefore referred to as the active structural acoustic control (ASAC) panel.

Due to the relatively high bending stiffness of the aluminium panel, the PVDF volume velocity actuator has a low control authority. Sutton et al. [13] calculated that a control voltage of 100 V_{rms} will yield a uniform pressure over the panel surface of 0.7 Pa. The aim of this study, however, is to investigate the principle of the PVDF volume velocity sensor/actuator pair. An alternative

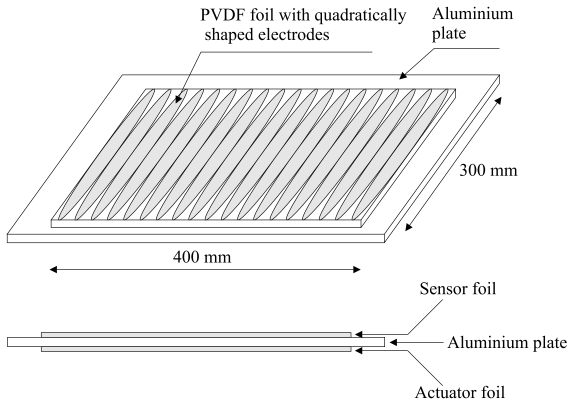

Fig. 3. Schematic view of the aluminium panel equipped with the actuator and sensor foil.

distributed acoustic actuator is described in Ref. [19]. A layer of PVDF is glued directly to a honeycomb core structure. The actuator has a bending stiffness which is comparable to the ASAC panel as discussed in this paper. However, the PVDF layers are placed at a distance of 3.2 mm from the neutral axis of the plate, and thus can apply a bending moment on the plate which is six times larger.

The actuation of the panel is done by one foil and is not symmetric with respect to the neutral axis of the panel. Consequently, the in-plane motion of the panel will be excited. Similarly, one foil is used as sensor, also sensing the in-plane vibration of the panel. Because of the high stiffness of the panel for the in-plane motion, a practical clamping of the panel is not stiff enough to prevent the in-plane motion of the panel. Consequently, this in-plane motion should be included in the model as given by the state space model [11,12]:

$$\begin{aligned}\dot{\mathbf{X}}_l(t) &= \mathbf{A}_l\mathbf{X}_l(t) + \mathbf{B}_{p,l}V_3(t) + \mathbf{B}_{m,l}\tilde{f}_m(t),\\ q_l(t) &= \mathbf{C}_l\mathbf{X}_l(t) + \mathbf{D}_{p,l}V_3(t) + \mathbf{D}_{m,l}\tilde{f}_m(t),\end{aligned} \tag{7}$$

with $q_l(t)$ the charge output due to the in-plane motion of the panel. The feedthrough matrices $\mathbf{D}_{p,l}$ and $\mathbf{D}_{m,l}$ are zero.

The charge output of the sensor foil $q(t)$ will be the summation of two contributions. First the contribution $q_b(t)$, proportional to the volume velocity $\Phi(t)$ of the panel:

$$q_b(t) = C_1\Phi(t) = \mathbf{C}_{b,1}\mathbf{X}_b(t). \tag{8}$$

Second the contribution $q_l(t)$ due to the in-plane motion of the panel. Models (4) and (7) are combined in the state space model for the ASAC panel:

$$\begin{aligned}\begin{bmatrix}\dot{\mathbf{X}}_b(t)\\ \dot{\mathbf{X}}_l(t)\end{bmatrix} &= \begin{bmatrix}\mathbf{A}_b & 0\\ 0 & \mathbf{A}_l\end{bmatrix}\begin{bmatrix}\mathbf{X}_b(t)\\ \mathbf{X}_l(t)\end{bmatrix} + \begin{bmatrix}\mathbf{B}_{p,b}\\ \mathbf{B}_{p,l}\end{bmatrix}V_3(t) + \begin{bmatrix}\mathbf{B}_{m,b}\\ \mathbf{B}_{m,l}\end{bmatrix}\tilde{f}_m(t),\\ q(t) &= [\,\mathbf{C}_{b,1} \quad \mathbf{C}_l\,]\begin{bmatrix}\mathbf{X}_b(t)\\ \mathbf{X}_l(t)\end{bmatrix}.\end{aligned} \tag{9}$$

The effect of the in-plane motion on the transfer function from voltage applied to the actuator to current output of the sensor foil is given in Fig. 4. The dashed line shows the transfer function

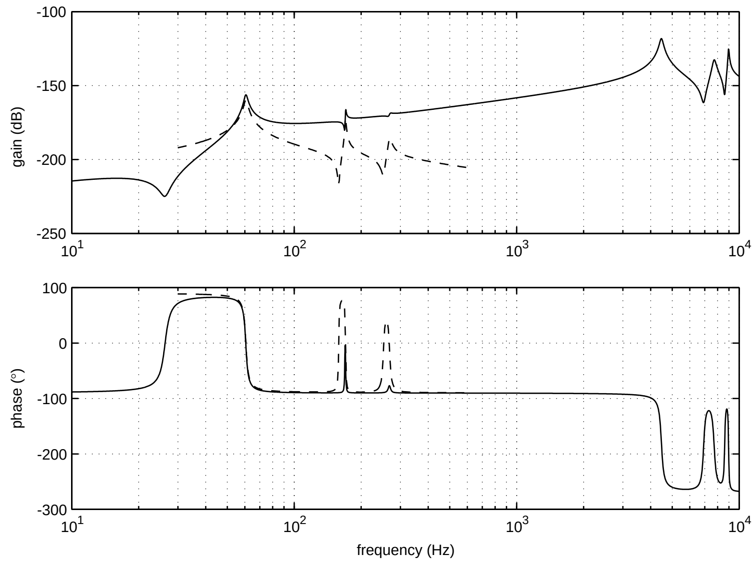

Fig. 4. Transfer function of the volume velocity sensor/actuator pair attached to ASAC panel (dashed line: without in-plane motion of the panel, solid line: with in-plane motion of the panel).

obtained when omitting the in-plane motion of the panel. Including the in-plane motion of the panel, however, will change this transfer function drastically, as shown by the solid line. The first in-plane resonance occurs at a frequency above 4000 Hz. The main problem lies in the phase of the transfer function which is not restricted to a band of -90° to $+90^\circ$. A direct velocity feedback control system is not unconditionally stable such that the main advantage of the collocated system is lost. At low frequencies the effect of the in-plane motion can be considered as a constant charge in the sensor output, which results in a current output that is increasing with 20 dB/dec. An additional zero occurs below the first structural resonance frequency.

Logically this has some consequences for the active control system in terms of stability and performance.

Stability: The phase of the open-loop transfer function is not limited between $+90^\circ$ and -90°. The system is not collocated and is not stable for any control gain. In addition, the amplitude is increasing with 20 dB/dec towards the first in-plane resonance frequency. Adding a low-pass filter to limit the amplitude of the transfer function at the first in-plane mode will cause the phase to cross -180° at a much lower frequency and destroy the phase margin of the controller.

Performance: The distance between the poles and zeros of the open-loop system is reduced even further due to the constant charge contribution. If a stable feedback control could have been designed, the root locus would have had smaller loops in the left half-plane and thus less active damping would have been achieved.

In order to include all effects that play a role in the coupling between the sensor and actuator foil, a finite element model was constructed. Piefort and Henrioulle [20] describe the construction of a fully coupled piezoelectric shell element that formed the basis to assemble a finite element model of the ASAC panel. The finite element model has proven capable of predicting accurately the open-loop transfer function of the collocated piezoelectric sensor/actuator pair, and therefore the performance of an active control system using this pair.

The conclusion is that direct velocity feedback, based on a system with the PVDF sensor/actuator pair is not feasible.

This paper discusses two solutions to this problem. First the volume velocity sensor is implemented as a discrete sensor, such that the in-plane motion is not measured. This sensor is discussed in the next section, and the volume velocity feedback control system in Section 4.5. Second, the PVDF volume velocity sensor/actuator pair is used in combination with a feedback controller that has some roll-off towards higher frequencies. This is the integral force feedback as presented in Section 4.3.

3.2. Discrete volume velocity sensor and PVDF volume velocity actuator

In order to test the direct velocity feedback approach, a discrete volume velocity sensor was built consisting of a grid of accelerometers placed on the ASAC panel. The acceleration in these points is summed and integrated to obtain an approximation of the volume velocity. Both the PVDF foils are used as volume velocity actuator, driven in opposite phase. The accelerometers do not measure the in-plane motion of the panel, and the transfer function between the PVDF volume velocity actuator and discrete volume velocity sensor will therefore be collocated in the low frequency range. This sensor should satisfy a number of conditions. In the frequency band where active damping is required, the signal should be a good approximation for the volume velocity of the panel. And for stability, the phase should lie between -90° and $+90^\circ$ in a much wider frequency band. Several possible locations for the accelerometers were simulated, and 12 locations that fulfil these conditions were selected.

The accelerometers (PCB 333A) weigh 5.6 g each, thereby adding mass to the panel and changing the dynamic properties of the panel. The measurement principle, however, does not depend on the properties of the panel such that this effect will not influence the design of the control system.

4. Experimental results

The discrete as well as the PVDF volume velocity sensor were implemented and tested in combination with the volume velocity actuator. In this paper, the effect of the control system on the sound transmission for normal incident sound is demonstrated. Under these conditions only the odd–odd structural modes will be excited by the incident sound field. Only these types of modes can be detected and controlled by the volume velocity sensor/actuator. As the incident sound field and the control action both apply a uniform sound pressure on the plate, the control system can—in theory—totally suppress the incident sound field. In practice, the reduction is limited by the stability of the control system, which is the major topic of this paper. As such the experiments will show the upper limit of the reduction that the control system can achieve. In the case of diffuse sound field excitation other types of structural modes will contribute to the sound transmission. As these modes are neither detectable nor controllable, they will remain unaffected after control. However, for a structure with a low modal density as in the current case, the sound transmission at low frequencies is largely determined by the first radiation mode of the structure [19]. As such the proposed control system is effective in suppressing the low frequency sound transmission through the panel.

4.1. Description of the test set-up

A test set-up was built to test the sound transmission loss through the ASAC panel, as shown in Fig. 5. The test set-up consists of a wooden box of thickness 18 mm. Inside this box a smaller box is placed. The gap of 25 mm between both is filled with sand. The sound transmission loss of the five walls of the box is 20 dB higher than that of the actively controlled ASAC panel. A loudspeaker inside the box excites the panel with plane sound waves. On top of the outer box a frame is placed on which the ASAC panel is mounted. This frame is not in contact with the inner box to prevent mechanical excitation of the frame due to the vibration of the loudspeaker. The dimensions of the inner box are chosen such that the acoustic modes of this box occur above 500 Hz, which is outside the frequency band of interest. The PVDF actuator foil is driven by an AVC790A01 power amplifier, the PVDF sensor foil is connected to a Kistler 5001 charge amplifier. The sound pressure is measured in a Brüel and Kjær 4188 microphone mounted in the centre of the panel at a distance of 20 cm from the panel. It is placed so close to the panel because of the very weak sound radiation from the panel due to the small control authority. At the first structural mode of the panel, the sound pressure in this microphone equals 50 dB for 1 V input to the volume velocity actuator. As the sound radiation in the low frequency range is quite uniform, the microphone signal is a good measure for the sound radiation of the panel.

4.2. PVDF volume velocity sensor/actuator pair

Fig. 6 shows the experimentally obtained transfer function between voltage input to the actuator foil and current output from the sensor foil. The first in-plane resonance occurs at about

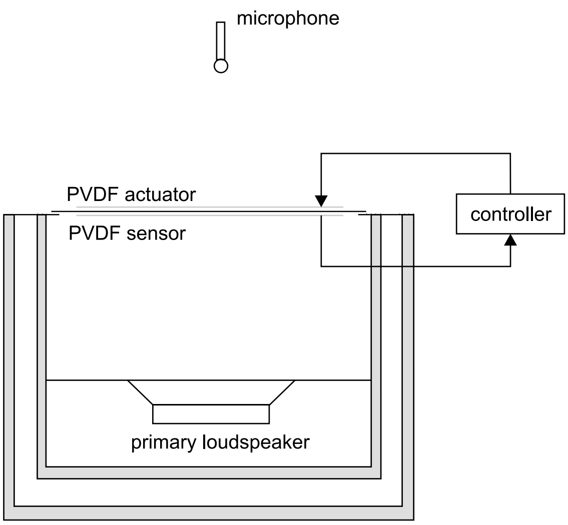

Fig. 5. Schematic view of the test set-up.

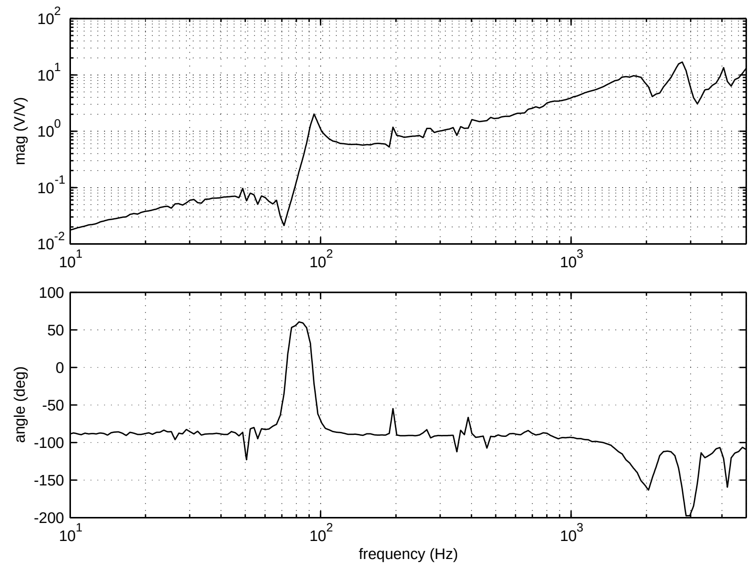

Fig. 6. Experimentally obtained transfer function of the PVDF sensor/actuator pair: voltage excitation to current output.

1800 Hz and the phase drops below -180° at this frequency. The measurement confirms the results of the simulations. The in-plane motion produces a constant contribution to the charge output of the sensor at low frequencies. The higher order bending modes cannot be distinguished in the sensor output, an additional zero is introduced at a frequency below the first structural mode and the distance between the zeros and poles is reduced.

4.3. Integral force feedback

Section 3.1 have shown that the signal from the PVDF volume velocity sensor cannot be used as feedback signal for direct velocity feedback control. Alternatively the charge signal from the PVDF sensor can be used as feedback signal. Instead of deriving the volume displacement signal to obtain the volume velocity of the panel, the volume displacement signal is integrated, and its sign is reversed as achieved by the compensator given in the equation

$$\mathscr{H}(s) = \frac{-g}{s}. \tag{10}$$

This way the phase of the feedback signal equals the phase of the direct volume velocity feedback control, but the amplitude will show a roll-off of -20 dB/dec, whereas the direct volume velocity feedback control showed an increase of $+20$ dB/dec. This way the in-plane modes, which occur at higher frequencies, will not be destabilized. In practice, a pure integrator will not be implemented as it is very sensitive for low frequency noise. The integral force feedback compensator for the ASAC panel will be implemented as a low-pass filter with cut-off frequency of 1 Hz which is well below the frequency range of interest.

This control strategy is described by Preumont [17] who used it to control a truss structure. In his approach, the force is measured by a piezoelectric force sensor, sent through the compensator

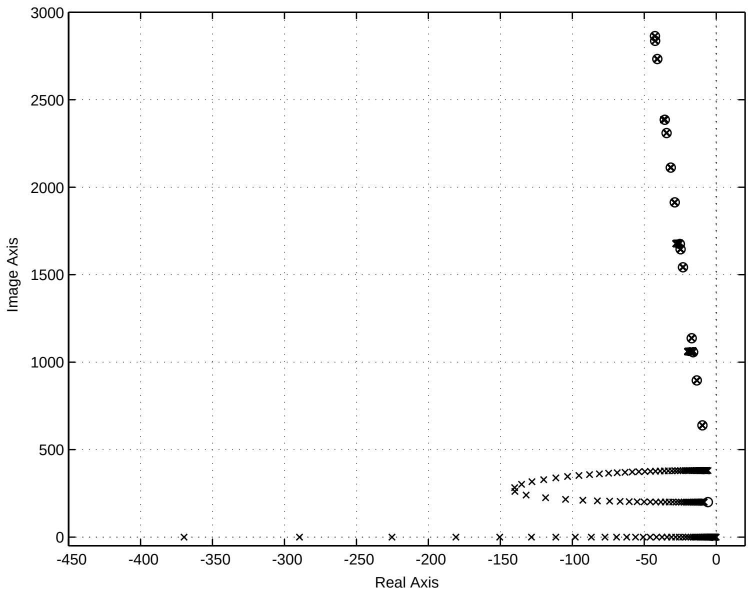

Fig. 7. Root locus of the integral force feedback controller.

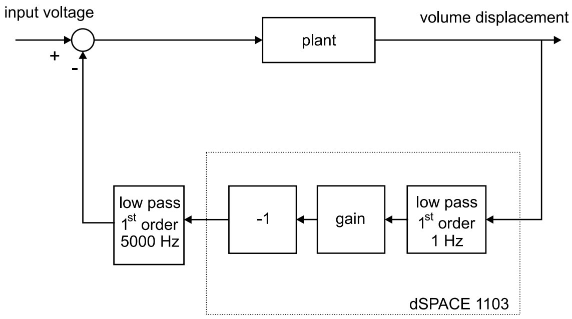

Fig. 8. Control scheme of the integral force feedback controller.

described above and feedback with a positive sign to a linear piezoelectric actuator. Therefore, this strategy is termed positive integral force feedback.

The root locus of the integral force feedback is shown in Fig. 7. Compared to the root locus of the direct volume velocity feedback in Fig. 2, the loops stretch much less into the left half-plane due to the reduced distance between the poles and the zeros of the controlled transfer function. In addition, the damping of the higher order modes is hardly increased due to the roll-off of the open-loop transfer function. The implementation of the integrator as a low-pass filter moves the compensator pole from the origin to the left on the real axis. Fig. 8shows the control scheme. The input for the plant, which is the aluminium panel equipped with the PVDF volume velocity sensor/actuator pair, is the voltage to the PVDF volume velocity actuator foil. The output is the charge output of the PVDF sensor foil. The integral force feedback control is implemented on a

Table 1
Open- and closed-loop poles for integral force feedback

Open loop		Closed loop	
ω (Hz)	ξ	ω (Hz)	ξ
94.0	0.032	77.5	0.129
192.4	0.011	191.4	0.014
260.5	0.012	260.1	0.015

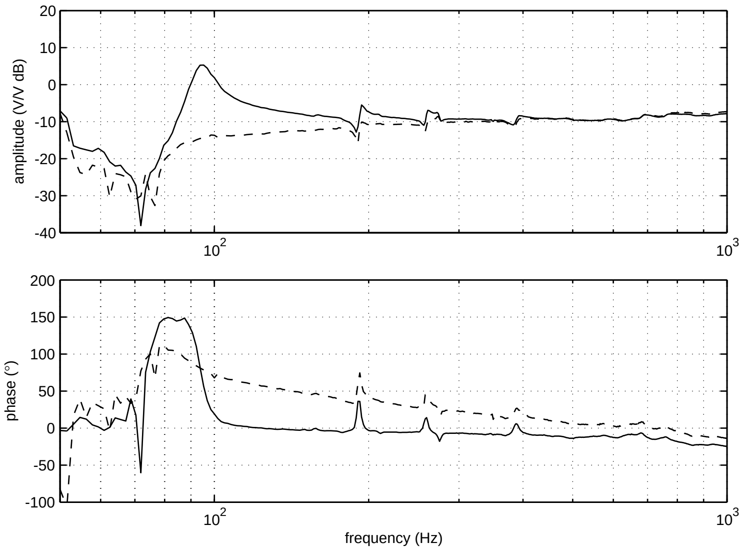

Fig. 9. Controlled transfer function from excitation voltage to volume displacement of the panel for integral force feedback (solid line: without control, dashed line: with control).

dSPACE 1103 control board, programmed with a simulink model. The sample frequency is 20 kHz. The output of the controller is filtered by a first order analog low-pass filter with a cut-off frequency of 5000 Hz to avoid high frequencies being sent to the PVDF actuator. The gain was chosen to yield a gain margin of 20 dB.

A model was fitted to the measured transfer function of the PVDF sensor/actuator pair, and used to calculate the open and closed-loop poles. These are listed in Table 1. The damping of the first structural mode is increased considerably, while the increase of the damping of the higher order modes remains limited. The controlled transfer function—that is from voltage input to the PVDF volume velocity actuator foil to the charge output of the PVDF volume velocity sensor foil—is shown in Fig. 9. It shows a reduction of more than 15 dB at the first structural resonance frequency. The reduction at higher order modes remains limited.

The final proof of the effectiveness of the control strategy is the measurement of the frequency response function from excitation of the loudspeaker to the sound pressure in the receiving room, as shown in Fig. 10. The reduction of the sound pressure output at the first resonance frequency

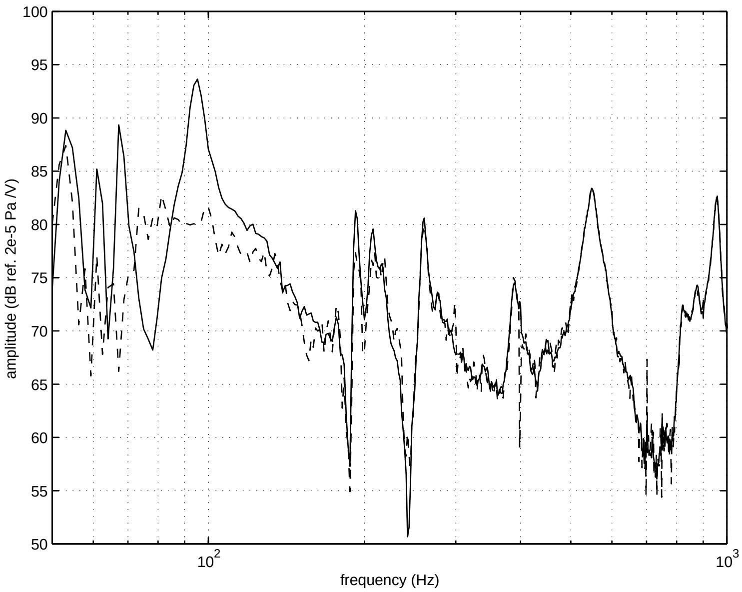

Fig. 10. Transfer function of loudspeaker voltage to sound pressure output for integral force feedback (solid line: without control, dashed line: with control).

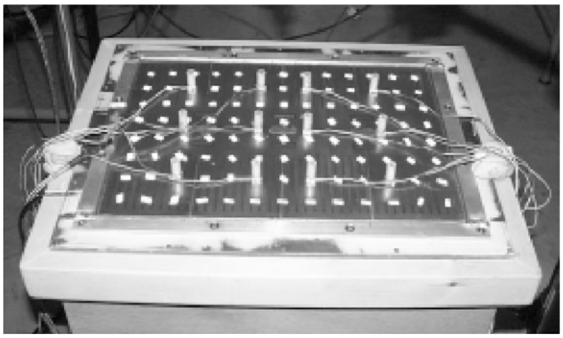

Fig. 11. Twelve accelerometers form a discrete volume velocity sensor.

amounts more than 10 dB, without spillover at other frequencies. Around 200 Hz some reduction can be observed.

4.4. Discrete volume velocity sensor and PVDF volume velocity actuator

Fig. 11 shows a picture of the discrete volume velocity sensor. The PVDF volume velocity actuator in combination with the discrete volume velocity sensor is still not perfectly collocated due to spatial aliasing. The open-loop transfer function between the PVDF volume velocity actuator and discrete volume velocity sensor—including a first order low-pass filter with a cut-off frequency of 500 Hz—is shown by the solid line in Fig. 12. Only below 700 Hz the phase is

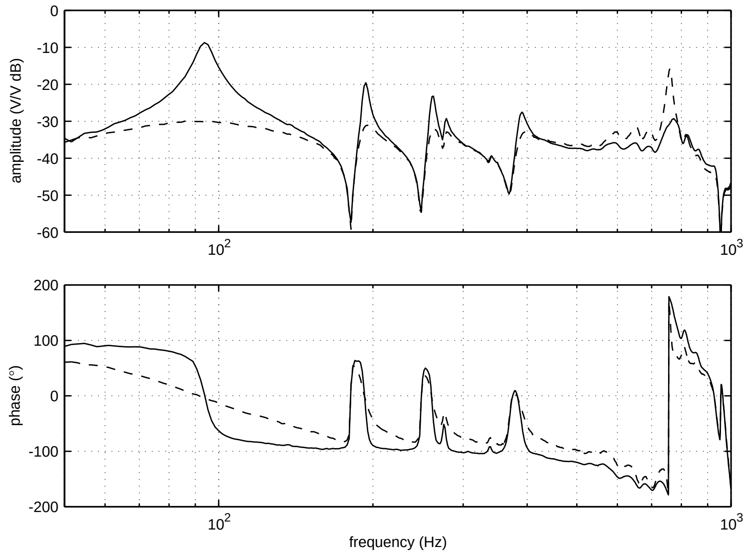

Fig. 12. Transfer function from excitation voltage to volume velocity of the panel for direct velocity feedback (solid line: without control, dashed line: with control).

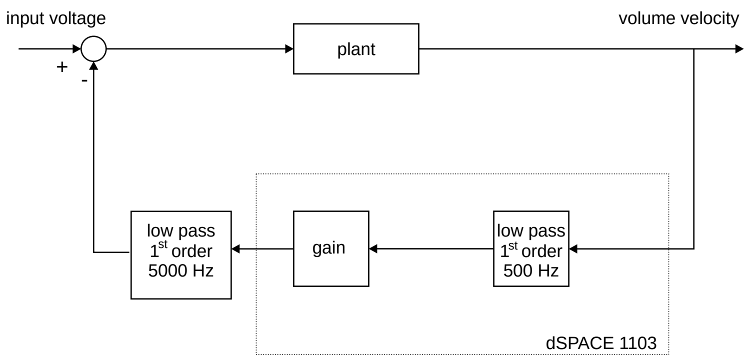

Fig. 13. Control scheme for the direct velocity feedback controller.

restricted between -90° and $+90^\circ$. However, the amplitude of the transfer function is decreasing for increasing frequencies, which was not the case for the PVDF volume velocity sensor/actuator pair. With the application of a low-pass filter, a stable volume velocity feedback controller can be constructed.

An electronic circuit was built to perform the summation and integration of the 12 accelerometer signals in real time, such that a feedback signal is available.

4.5. Direct volume velocity feedback

The discrete volume velocity sensor allows the implementation of a direct velocity feedback controller which is depicted in Fig. 13. The compensator consists of a first order low-pass filter

Table 2
Open- and closed-loop poles for direct volume velocity feedback

Open loop		Closed loop	
ω (Hz)	ξ	ω (Hz)	ξ
93.9	0.029	90.6	0.348
193.2	0.009	189.8	0.034
261.2	0.001	257.7	0.027
389.5	0.014	386.6	0.028

with a cut-off frequency of 500 Hz and a gain. The input for the plant is the voltage to the PVDF volume velocity actuator, consisting of both the PVDF foils driven in opposite phase. The output is the voltage from the electronic circuit processing the signal from the 12 accelerometers on the panel. In order to increase the roll-off of the controller towards higher frequencies, the output of the volume velocity sensor is passed through a first order low-pass filter with a cut-off frequency of 500 Hz. This filter and the feedback gain are implemented on a dSPACE 1103 control board, and run at a sample frequency of 20 kHz.

The controlled transfer function is shown by a dashed line in Fig. 12. The amplitude at the first structural resonance frequency is reduced by 20 dB. It resembles very well the simulated closed-loop transfer function shown in Fig. 1. At a frequency of 750 Hz, that is where the phase crosses -180°, the amplitude of the transfer function is increased. This can be avoided by using more accelerometers to construct the discrete volume velocity sensor, at the expense of a more complicated sensor. Similarly as for the integral force feedback, the open and closed-loop poles were calculated and are listed in Table 2. The damping of the first structural mode is increased by a factor of 10. The damping of the other controlled modes, which are all (odd, odd) modes, is more than doubled.

Fig. 14 shows that the sound pressure in the receiving room at the first resonance frequency is reduced by more than 15 dB. A reduction up to 10 dB is achieved at the second and third resonance frequencies. Generally, the sound pressure in the frequency band below 300 Hz is reduced considerably without spillover at higher frequencies, except at a frequency of 750 Hz as discussed above.

5. Conclusions

Active control of volume velocity is an efficient control strategy to control the low frequency sound transmission through a rectangular panel. The control system can be implemented as a single-input single-output controller using a volume velocity sensor and volume velocity actuator. They form a collocated sensor/actuator pair such that the open-loop transfer function is minimum phase. Consequently, simple and efficient feedback control strategies can be implemented. Moreover, the sensing and actuation of the volume velocity does not depend on the mechanical properties of the panel.

A first control system applying this principle uses a PVDF distributed volume velocity sensor as well as a PVDF distributed volume velocity actuator. When used in a configuration that is not

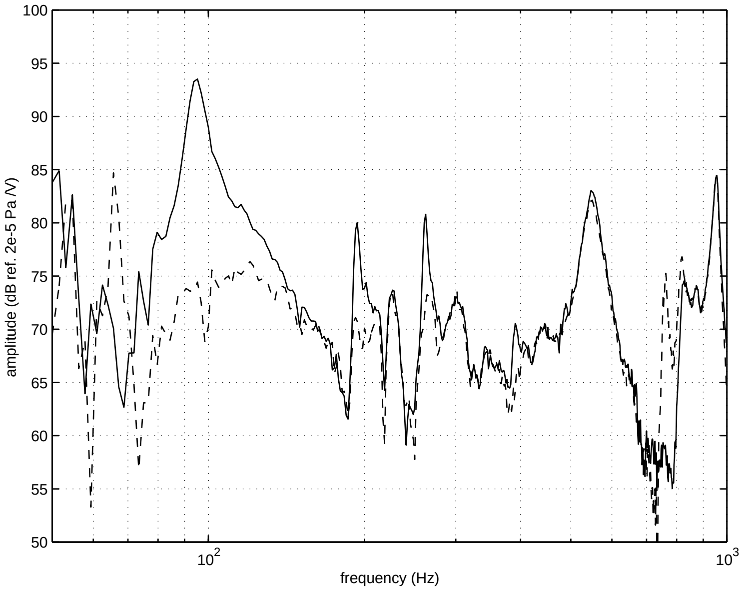

Fig. 14. Frequency response function of loudspeaker voltage to sound pressure output for direct velocity feedback (solid line: without control, dashed line: with control).

symmetric with respect to the neutral axis of the panel, the in-plane motion of the panel is excited by the actuator and measured by the sensor such that the open-loop transfer function is not minimum phase. The advantageous properties of the collocated sensor/actuator pair are lost. An integral force feedback control system is applied, providing roll-off towards higher frequencies, thereby not destabilizing the in-plane modes of the panel. A reduction of 5–10 dB is observed in the sound pressure measured in the receiving room in the frequency range from 0 to 200 Hz, without spillover to higher frequencies.

A second control system was implemented using a discrete volume velocity sensor, consisting of a grid of accelerometers, and a distributed volume velocity actuator, consisting of two PVDF foils driven in opposite phase. These form a collocated volume velocity sensor/actuator pair to which direct velocity feedback is applied. Experimental results show a reduction of 10–15 dB in the sound pressure in the receiving room in the frequency range from 0 to 300 Hz, again without spillover to higher frequencies.

Acknowledgements

The work reported herein was related to the EC Brite/Euram Research Project DAFNOR (under contract BRPR-CT96-0154). The project is supported by the Directorate-General for Science; Research and Development of the CEC.

This paper presents research results of the Belgian programme on Interuniversity Poles of Attraction initiated by the Belgian State, Prime Minister's Office, Science Policy Programming. The scientific responsibility is assumed by its authors.

References

[1] G.V. Borgiotti, The power radiated by a vibrating body in an acoustic fluid and its determination from boundary measurements, Journal of the Acoustical Society of America 88 (1998) 1884–1893.

[2] Z. Li, C. Guigou, C.R. Fuller, R.A. Burdisso, Design of active acoustic control systems using a nonvolumetric eigenproperty assignment approach, Journal of the Acoustical Society of America 101 (4) (1997) 2088–2096.

[3] M.E. Johnson, S.J. Elliott, Volume velocity sensors for active control, Proceedings of the Institute of Acoustics 15 (3) (1993) 411–420.

[4] A.P. Berkhoff, Sensor scheme design for active structural acoustic control, Journal of the Acoustical Society of America 108 (3) (2000) 1037–1045.

[5] C. Guigou, A. Berry, F. Charette, J. Nicolas, Active control of beam volume velocity using shaped PVDF sensor, Acustica 82 (1996) 772–783.

[6] F. Charette, A. Berry, C. Guigou, Active control of sound radiation from a plate using a PVDF volume displacement sensor, Journal of the Acoustical Society of America 103 (3) (1998) 1493–1503.

[7] S.D. Snyder, N. Tanaka, Y. Kikushima, The use of optimally shaped piezo-electric film sensors in the active control of free field structural radiation, Part 1: feedforward control, Journal of Vibration and Acoustics 117 (1995) 311–322.

[8] S.D. Snyder, N. Tanaka, Y. Kikushima, The use of optimally shaped piezo-electric film sensors in the active control of free field structural radiation, Part 2: Feedback control, Journal of Vibration and Acoustics 118 (1996) 112–121.

[9] M.E. Johnson, S.J. Elliott, Active control of sound radiation using volume velocity cancellation, Journal of the Acoustical Society of America 98 (4) (1995) 2174–2186.

[10] K. Henrioulle, P. Sas, DAFNOR Distributed Active Foils for NOise Reduction—a project overview, ISMA25—International Conference on Noise and Vibration Engineering, Leuven, Belgium, 2000, pp. 845–854.

[11] P. Gardonio, Y.S. Lee, S.J. Elliott, S. Debost, Active control of sound transmission through a panel with a matched PVDF sensor and actuator pair, ACTIVE99, Fort Lauderdale, USA, December 1999.

[12] P. Gardonio, Y.S. Lee, S.J. Elliott, S. Debost. Design of a panel with matched PVDF volume velocity sensor and uniform force actuator pair, ISMA25 International Conference on Noise and Vibration Engineering, Leuven, Belgium, September 2000, pp. 833–844.

[13] T.J. Sutton, M.E. Johnson, S.J. Elliott, A distributed actuator for the active control of sound transmission through a partition. Sixth Conference on Recent Advances in Structural Dynamics, Southampton, July 1997, pp. 1247–1255.

[14] L. Meirovitch, Elements of Vibration Analysis, McGraw-Hill, New York, 1975.

[15] A. Leissa, Vibration of plates, Acoustical Society of America, Melville, NY, 1993.

[16] S.J. Elliott, M.E. Johnson, Radiation modes and the active control of sound power, Journal of the Acoustical Society of America 94 (4) (1993) 2194–2204.

[17] A. Preumont, Vibration Control of Active Structures, Kluwer, Dordrecht, 1997.

[18] M.L. Fripp, M.J. Atalla, Review of modal sensing and actuation techniques, The Shock and Vibration Digest 33 (1) (2001) 3–14.

[19] K. Henrioulle, Distributed Actuators and Sensors for Active Noise Control. Ph.D. Thesis, KULeuven, Department of Mechanical Engineering, Leuven, Belgium, October 2001.

[20] V. Piefort, K. Henrioulle, Modelling of smart Structures with collocated piezoelectric actuator/sensor pairs: influence of the in-plane components. Fifth International Conference on Computational Structures Technology, Leuven, Belgium, September 2000, pp. 47–58.